

## Domain structure evolution in relaxor PLZT 8/65/35 ceramics after chemical etching and electron beam irradiation

L. V. Gimadeeva, V. A. Shikhova, D. S. Chezganov, A. S. Merzliakova, E. O. Vlasov, V. V. Fedoroviyh, A. L. Kholkin, B. Malič & V. Ya. Shur

To cite this article: L. V. Gimadeeva, V. A. Shikhova, D. S. Chezganov, A. S. Merzliakova, E. O. Vlasov, V. V. Fedoroviyh, A. L. Kholkin, B. Malič & V. Ya. Shur (2018) Domain structure evolution in relaxor PLZT 8/65/35 ceramics after chemical etching and electron beam irradiation, *Ferroelectrics*, 525:1, 83-92, DOI: [10.1080/00150193.2018.1432933](https://doi.org/10.1080/00150193.2018.1432933)

To link to this article: <https://doi.org/10.1080/00150193.2018.1432933>



Published online: 15 Mar 2018.



Submit your article to this journal [↗](#)



Article views: 3







View related articles [↗](#)



View Crossmark data [↗](#)



# Domain structure evolution in relaxor PLZT 8/65/35 ceramics after chemical etching and electron beam irradiation

L. V. Gimadeeva<sup>a</sup>, V. A. Shikhova <sup>a</sup>, D. S. Chezganov <sup>a</sup>, A. S. Merzliakova<sup>a</sup>, E. O. Vlasov<sup>a</sup>, V. V. Fedorovych<sup>a</sup>, A. L. Kholkin <sup>a,b</sup>, B. Malič<sup>c</sup>, and V. Ya. Shur <sup>a</sup>

<sup>a</sup>School of Natural Sciences and Mathematics, Ural Federal University, Ekaterinburg, Russia; <sup>b</sup>Department of Physics & CICECO-Aveiro Institute of Materials, University of Aveiro, Aveiro, Portugal; <sup>c</sup>Ceramics Department of Jozef Stefan Institute, Ljubljana, Slovenia

## ABSTRACT

Domain structure and its evolution on the surface of PLZT 8/65/35 ceramics after selective chemical etching and e-beam irradiation was studied. It is shown that the initial mixture of the nanoscale fractal-type 3D maze (fractal dimension 2.8) and micron-size domains turned into lamellar domains with periods ranging from 100 to 800 nm as a result of such procedures. The observed etch-induced change of the domain structure was attributed to the action of the depolarization field after partial removing the screening charges. The dependence of the switched domain area on irradiation time (dose) was measured in e-beam irradiated samples.

## ARTICLE HISTORY

Received 30 August 2017  
Accepted 27 November 2017

## KEYWORDS

Relaxor ferroelectrics; piezoresponse force microscopy; selective chemical etching; polarization reversal; electron beam irradiation; domain structures

## 1. Introduction

Ferroelectrics with a diffuse phase transition, which exhibit an abnormal frequency dependence of the dielectric constant, are called relaxor ferroelectrics or relaxors [1]. Relaxors, in contradiction to classical ferroelectrics, have high values of susceptibilities (dielectric, electro-optical, piezoelectric, etc.) in an abnormally wide temperature range; thus, these materials are widely used in optical devices (e.g. modulators), actuators, sensors, and transducers [1]. Relaxors are disordered ferroelectrics with the nanoscale quasi-regular maze domain structure appeared after cooling below freezing temperature [2–7]; such domains were also called “finger-print domains” [4,5], “labyrinth-type nanoscale domains” [6], or “square-patched domains” [7]. The unique properties of relaxor ferroelectrics raised fundamental interest in understanding the mesoscopic domain structures in these materials, including micro- and nano-domain populations, polarization distributions, and their evolution under external electric field and temperature variations. Transparent relaxor ceramics of lanthanum doped lead zirconate-titanate (PLZT) were first obtained and studied in 1980s [8]. The advantages of PLZT ceramics are high optical transparency and electro-optical coefficients [9]. The modern ceramic technology is less expensive and allows producing large blocks of complex solid solution, thus making the ceramics optimal for solving many scientific and

**CONTACT** L. V. Gimadeeva  [lv.gimadeeva@urfu.ru](mailto:lv.gimadeeva@urfu.ru)

Color versions of one or more of the figures in the article can be found online at [www.tandfonline.com/gfer](http://www.tandfonline.com/gfer).

© 2018 Taylor & Francis Group, LLC

technical problems [9]. PLZT was successfully used in segment displays, optical closures, coherent modulators, color filters, image storage devices, etc. [9].

Static domain patterns visualized using Piezoresponse Force Microscopy (PFM) in PLZT  $x/65/35$  ( $x = 6\text{--}9.75\%$ ) ceramics after zero-field-cooling below the freezing temperature showed a nanoscale quasi-regular maze (“finger-print” pattern) with average periods from 30 to 220 nm [4,5]. Complex domain structure observed in PLZT 9.75/65/35 ceramics was attributed to a La-induced disorder and a correlation length of about 50 nm was determined using autocorrelation processing of the PFM images [10]. Grain size effect in PLZT 9.75/65/35 was attributed to inhomogeneous distribution of the correlation length and disorder increasing at the grain boundaries [11]. It was shown that the correlation length of the domain patterns decreased with increasing La content, being sensitive also to the synthesis method [12]. The behavior of the correlation length was linked to the macroscopic properties, showing a strong increase of disorder with La doping [12].

The polarization reversal in relaxor PLZT  $x/65/35$  ( $x = 5\text{--}12\%$ ) ceramics was traditionally studied using macroscopic methods: recording of hysteresis loops, switching currents in saw type electric field [13, 14], and elastic light scattering [15]. The qualitative difference of the shape of the switching current above and below freezing temperature was attributed to spontaneous backswitching in relaxor phase under the action of the depolarization field produced by the bound charges located at the interphase boundaries [13, 14].

The domain visualization by channeling-contrast backscattered electron microscopy in PLZT  $x/65/35$  ceramics ( $1 < x < 10$ ) allowed revealing the influence of La concentration and electric field poling on the domain structure geometry [7, 16]. It was shown that the lamellar domain structure appeared in ferroelectric (at room temperature) compositions and “square-patched” pattern in relaxors in unpoled and *ex-situ* poled samples [7]. The domain pattern of the unpoled samples changed from lamellar domains with various orientations within a single grain (1/65/35) towards a maze domain pattern, where domains decreased in size with increasing La content [7]. The domain structure changed from a maze pattern to a lamellar one for  $1 < x < 7$  [7]. No domain changes were detected in the relaxor compositions [7].

The influence of the chemical etching on the ferroelectric domain structure is a well-known in ferroelectrics [17, 18]. The rearrangement of the domain structure induced by selective chemical etching (pure HF) observed in periodically poled MgO-doped stoichiometric lithium tantalate single crystals was attributed to partial backswitching under the action of depolarization field after removing the surface layer with screening charges [17].

In this work, we have compared the initial domain structures and structures appeared after selective chemical etching and electron beam (e-beam) irradiation in PLZT 8/65/35 ceramics in order to understand the mechanism of domain formation in these materials.

## 2. Experimental

The studied  $\text{Pb}_{1-x}\text{La}_x(\text{Zn}_{0.65}\text{Ti}_{0.35})_{1-x/4}\text{O}_3$  ceramics (PLZT 8/65/35) were sintered by the hot pressing method at the Ceramics Department of Jozef Stefan Institute, Ljubljana, Slovenia [19]. After thermal depolarization, 0.77-mm-thick samples were polished to the optical quality with a gradual decrease of diamond abrasive down to  $0.25\text{ }\mu\text{m}$  and mechanochemical strain-free polishing by colloidal silica (particle size below 100 nm) [20]. Thermal depolarization was carried out during cooling from  $200^\circ\text{C}$  to room temperature with cooling rate  $5^\circ\text{C}/\text{min}$  without electric field. Two types of the surface treatments have been applied in order to change the surface domain structure: selective chemical etching and e-beam scanning.

## 2.1. Chemical etching

The used etchants consisted of Buffered Oxide Etch (BOE), Nitric acid ( $\text{HNO}_3$ ), Hydrochloric acid (HCl), and deionized (DI) water [21]. Three variants of the sample etching procedure have been used.

**The first etching variant** consisted of four stages: (1) etching in acid mixture (1 part of BOE, 2 parts of HCl, and 3 parts of DI water) for few seconds; (2) immersion in DI water; (3) removal of the precipitated film formed in the etching process by 50% solution of  $\text{HNO}_3$ ; and (4) completion of chemical processes by repeated washing in DI water [21].

**The second etching variant** consisted of three stages without sample immersion in deionized water between the first and the third stages.

**The third etching variant** consisted of four stages using the acid mixture additionally diluted with DI water to the ratio 1 BOE: 2 HCl: 9 DI water for reducing the etching rate.

**E-beam irradiation** was performed by continuous surface scanning by electron beam with 10 nm diameter, accelerating voltage 10 kV, e-beam current 1 nA, and irradiation doses 30–90  $\mu\text{C}/\text{cm}^2$  [22]. The dose is total charge of incident beam exposed during a certain time interval  $D = (I \cdot t_{\text{irr}})/A_{\text{irr}}$ , where  $I$  is e-beam current,  $t_{\text{irr}}$  is the irradiation time,  $A_{\text{irr}}$  is irradiated area. The scanning electron microscope (SEM) Auriga CrossBeam workstation (Carl Zeiss NTS, Germany) with Schottky field emission gun equipped with the e-beam lithography (EBL) system Elphy Multibeam (Raith GmbH, Germany) was used. The design was specified by Raith Nano-suite software.

The created domain structure was visualized by various high resolution methods: (1) SEM and atomic force microscopy (AFM) after selective chemical etching, and (2) PFM without etching after e-beam irradiation.

Selective chemical etching is one of the most popular methods used for revealing the surface domain patterns in ferroelectrics. The inherent significant difference in the etching rate for different domains leads to formation of the surface relief with steps at the domain walls. SEM operated at 3 kV accelerating voltage in the secondary electron detection mode allowed achieving the resolution down to 2 nm [23].

A scanning probe microscope (SPM) NTEGRA Aura (NT-MDT SI, Russia) with silicon tips with a diamond-like conductive coating was used. AC excitation voltage  $U_{\text{mod}}$  with amplitude 1–10 V and frequency about 400 kHz was applied between the conductive tip and the solid bottom electrode in order to induce the piezoelectric response. The obtained amplitude and phase of the PFM signal provided information about the domain structure on the surface layer. The estimated lateral resolution was below 50 nm. During the SPM measurements, I-shaped NSC/Pt 18 probes (MikroMasch, Estonia), coated with a conductive layer of platinum with the tip radius below 35 nm, resonant frequency of oscillations of 265–400 kHz, and a power constant of 20–75 N/m were used.

## 3. Results and discussion

### 3.1. Initial domain structure after polishing

The initial domain structure obtained after thermal depolarization and subsequent polishing was visualized by PFM (Fig. 1). The typical surface roughness was about 2 nm. The domain structure represented a mixture of the nanoscale fractal-type 3D maze and micron-size domain structures. The formation of fractal-type 3D maze structure is typical for PLZT

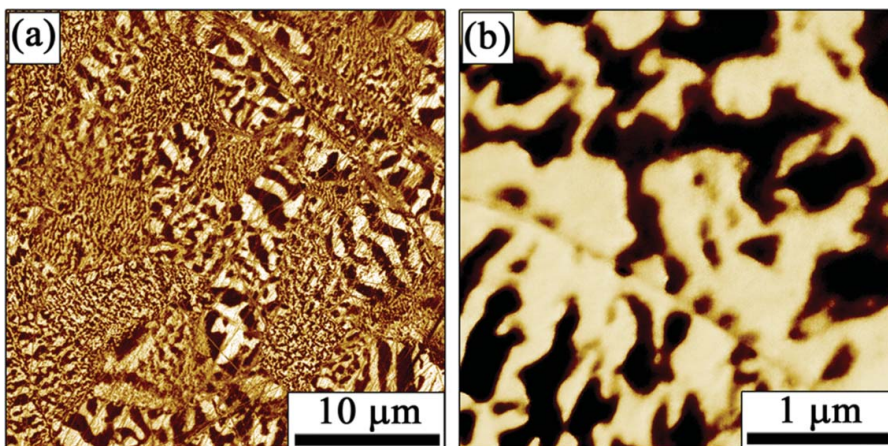


**Figure 1.** PFM images of the initial domain structure in PLZT 8/65/35 after polishing. Signal phase. Phase image is shown with phase varying from 0 and 180° in bright and dark areas.

8/65/35 samples after thermal depolarization [4, 5, 12]. The fractal dimension  $D_{HB}$  of the maze structure defined by box-counting method was about 2.8 [24]. The autocorrelation function allowed revealing the average correlation radius of maze structure about 160 nm [25].

The formation of micron-size domain structures in some grains (Fig. 1b) can be attributed to the removal of the surface layer of screening charges during the polishing process and backswitching under the action of residual depolarization field [17].

### 3.2. Domain structure after chemical etching

The typical images of the surface domain structure were obtained by SEM and AFM after the second etching variant performed in three stages. In this case, the maze type structure similar to the initial one with surface roughness about 70 nm was obtained (Fig. 2).

The images of the domain structure after the first variant of the chemical etching performed in four stages were obtained by SEM and AFM (Fig. 3). The coexistence of maze-type and lamellar domain structures appeared in this case. Moreover, some etching

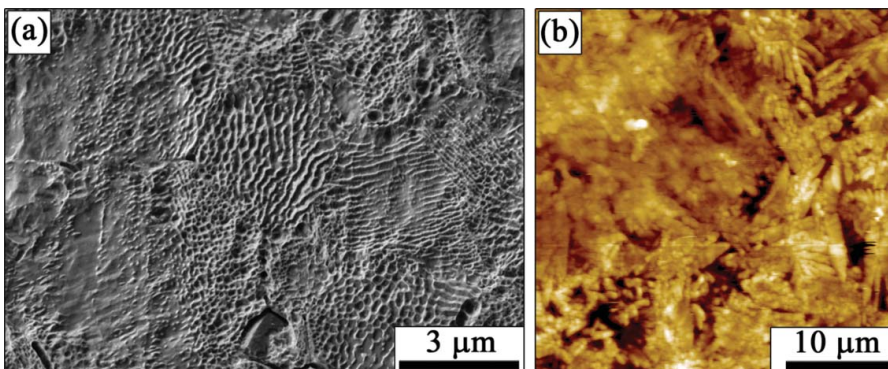


**Figure 2.** (a) SEM and (b) AFM images of the domain structure after the second variant of chemical etching performed in three stages.



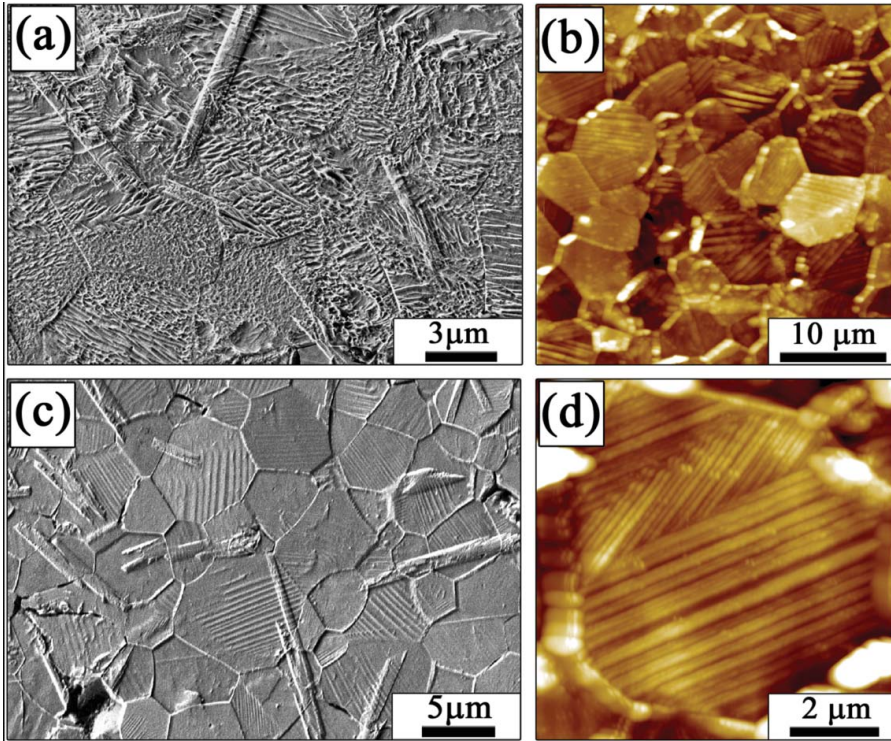


**Figure 3.** (a, b) SEM and (c, d) AFM images of the domain structure after the first variant of chemical etching performed in four stages.

by-products appeared on the surface. The period of lamellar domain structures varies from 120 to 860 nm and the surface roughness was about 20 nm.

The observed etch-induced change of the domain structure can be attributed to the action of the depolarization field after partial removing of the screening charges by etching [17]. In contrast to the three stage etching process, the essential deceleration of the external screening in the insulating DI water led to the increase of the residual depolarization field. Thus, the absence of the immersion in DI water in three stage etching variant reduced the depolarization field value and the polarization reversal did not occur.

The third etching variant occurred in four stages using the additionally diluted acid mixture led to the most effective change of the initial domain structure to the lamellar one with various lamellar orientations within each grain (Fig. 4). The rarely observed propagations of the lamellar domains through the grain boundary can be attributed to the similar crystallographic orientation in neighboring grains (low-angle grain boundaries) (Fig. 4d). The obtained roughness was about 30 nm. The period of lamellar domain structures varied from 140 to 570 nm.

### 3.3. Domain structure after e-beam irradiation

The sample with initial domain structure was irradiated by scanning with a focused e-beam under various doses. The comparison of the domain images in various regions before

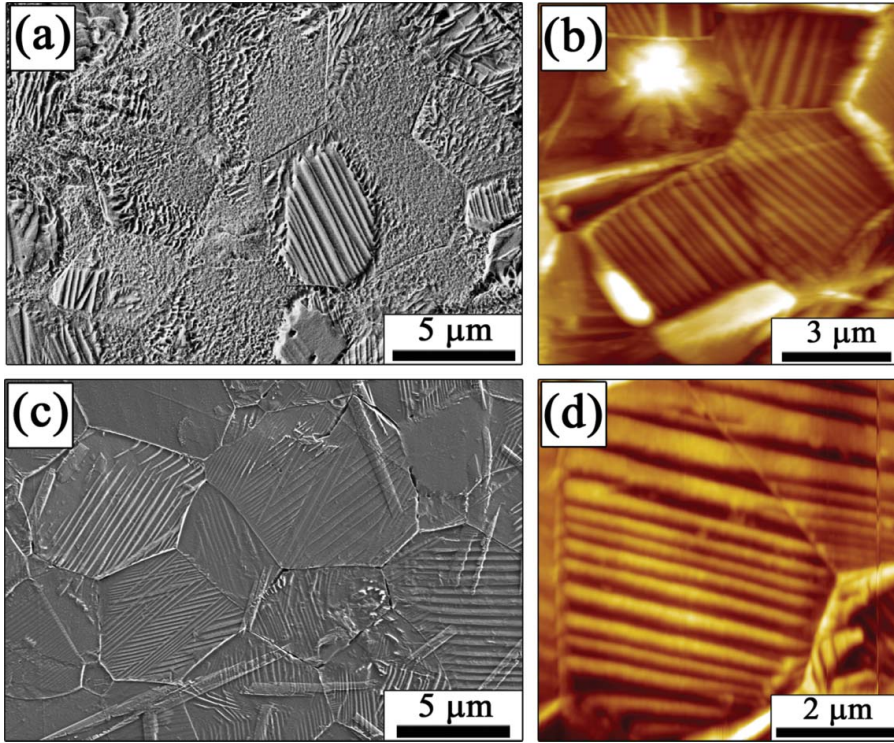


**Figure 4.** (a, b) SEM and (c, d) AFM images of the relief of the domain structure in PLZT after the third variant of chemical etching with additionally diluted acid mixture.

(Fig. 5a-c) and after (Fig. 5d-i) e-beam scanning allowed revealing the domain size increase and formation of the lamellar structures observed in the lateral PFM signal.

Appearance of 180° and 90°-oriented domain walls can be attributed to different grain orientation. The period of the lamellar domain structures varied from 100 nm to 1 μm.

The comparison of the PFM domain images for the same location before and after e-beam irradiation allowed to measure the dependence of the relative switched area on irradiation time (dose)  $\Delta q(t_{irr}) = [A(t_{irr}) - A_0]/A$ , where  $A_0$  and  $A(t_{irr})$  are the domain areas before and after irradiation (Fig. 6). The experimental points were fitted by:

$$\Delta q(t_{irr}) = \Delta q_{max}(1 - \exp(-t_{irr} / \tau_{eff})) \quad (1)$$

where  $\Delta q_{max} = \Delta A_{max}/A$  is the maximum value of the relative switched area,  $A$  is the area of PFM image,  $\tau_{eff}$  is the characteristic time.

The used fitting formula is based on the known dependence of the surface potential on the irradiation time  $V_s(t_{irr})$  for charging of insulators under irradiation with medium-energy electron beams [26, 27].

$$V_s(t_{irr}) = V_{ss}(1 - \exp(-t_{irr} / \tau_{eff})) \quad (2)$$

where  $V_{ss}$  is the maximum (steady-state equilibrium) value of the surface potential.



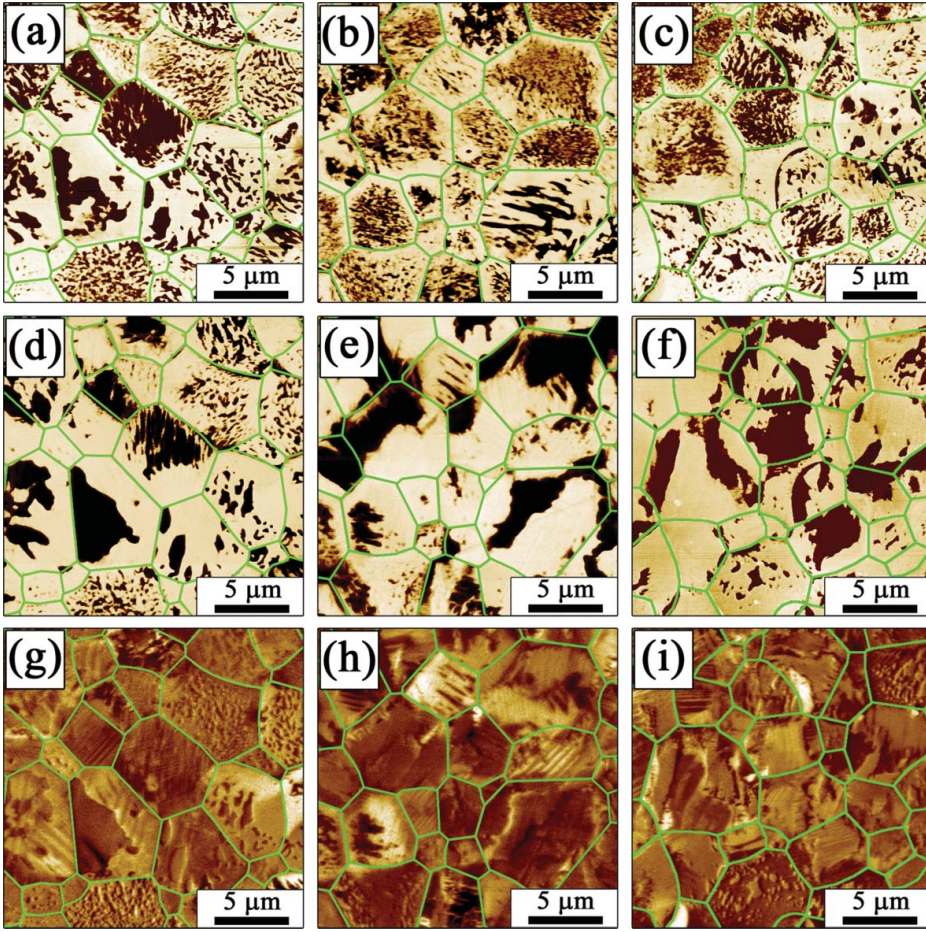


**Figure 5.** PFM domain images: (a-c) initial state (vertical signal); after e-beam irradiation (d-f) vertical signal and (g-i) lateral signal. Irradiation doses: (d,g)  $30 \mu\text{C}/\text{cm}^2$ , (e,h)  $60 \mu\text{C}/\text{cm}^2$ , (f,i)  $90 \mu\text{C}/\text{cm}^2$ . Grain boundaries marked by green lines. Accelerating voltage 10 kV.

This effect leads to saturation of the switched area for polarization reversal by e-beam irradiation for proper accelerated voltage. In our experiment for accelerating voltage 10 kV we obtain the following values of the fitting parameters:  $\Delta q_{\text{max}} = 0.16$  and  $\tau_{\text{eff}} = 4.7$  s. Thus for used values of e-beam current and accelerated voltage only 16% of the irradiated area can be switched even for infinite irradiation time in studied PLZT ceramics.

#### 4. Conclusion

We have studied the initial surface domain structure in PLZT 8/65/35 ceramics and its evolution as a result of selective chemical etching and e-beam irradiation. The initial domain structure represented a mixture of the nanoscale fractal-type maze. Micron-size domain structures were characterized by fractal dimension ( $D_{\text{HB}} = 2.8$ ) and average correlation length 160 nm. The almost complete change of the initial domains to the lamellar domain structure was observed as a result of chemical etching. Differently oriented lamellar domains



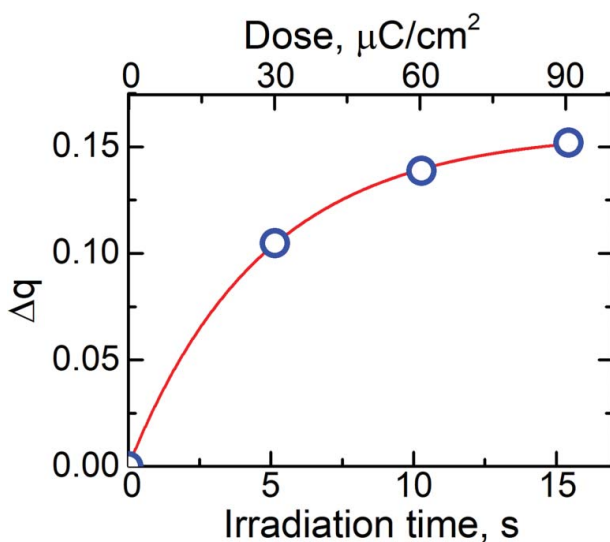


**Figure 6.** The dose dependence of the relative switched area. Accelerating voltage 10 kV.

within single grain were identified. We infer that the observed etch-induced change of the domain structure is invoked by the residual depolarization field increased as a result of partial removing of the screening charges during etching. The e-beam irradiation led to formation of the lamellar domains in some grains and increase of the domain area (partial polarization reversal). The analysis of PFM images allowed characterizing the domain structures evolution as a result of e-beam irradiation with different doses.

## Acknowledgment

The equipment of the Ural Center for Shared Use “Modern nanotechnology” Ural Federal University was used.

## Funding

Russian Foundation of Basic Research (Grant 16-02-00821-a). The Government of Russian Federation (Act 211, Agreement 02.A03.21.0006). The Ministry of Education and Science of the Russian Federation (Project No. 1366.2014/236). The project CICECO-Aveiro Institute of Materials (POCI-01-0145-FEDER-007679, FCT Ref. UID/CTM/50011/2013), financed by national funds through the FCT/MEC and, when appropriate, co-financed by FEDER under the PT2020 Partnership Agreement.

## ORCID

V. A. Shikhova  <http://orcid.org/0000-0002-5612-6222>  
 D. S. Chezganov  <http://orcid.org/0000-0001-8696-262X>  
 A. L. Kholkin  <http://orcid.org/0000-0003-3432-7610>  
 V. Ya. Shur  <http://orcid.org/0000-0002-6970-7798>

## References

- [1] G. A. Samara, The relaxational properties of compositionally disordered  $\text{ABO}_3$  perovskites. *J Phys: Condens Matter*. **15**, R367–R411 (2003).
- [2] V. Ya. Shur, Kinetics of polarization reversal in normal and relaxor ferroelectrics: relaxation effects. *Phase Transitions*. **65**, 49–72 (1998).
- [3] J. Dec, V. V. Shvartsman, and W. Kleemann, Domain-like precursor clusters in the paraelectric phase of the uniaxial relaxor  $\text{Sr}_{0.61}\text{Ba}_{0.39}\text{Nb}_2\text{O}_6$ . *Appl Phys Lett*. **89**, 212901 (2006).
- [4] E. V. Nikolaeva, V. Ya. Shur, E. I. Shishkin, and A. Sternberg, Nanoscale domain structure in relaxor PLZT x/65/35 ceramics. *Ferroelectrics* **340**, 137–143 (2006).
- [5] V. V. Shvartsman, A. Orlova, D. Kiselev, A. Sternberg, and A. L. Kholkin, Direct observation of polar nanostructures in PLZT ceramics for electrooptic applications. *Mat Res Soc Symp Proc*. **838E**, O4.16 (2005).
- [6] N. A. Pertsev, D. A. Kiselev, I. K. Bdikin, M. Kosec, and A. L. Kholkin, Quasi-one-dimensional domain walls in ferroelectric ceramics: Evidence from domain dynamics and wall roughness measurements. *J Appl Phys*. **110**, 052001 (2011).
- [7] M. Otonicar, A. Reichmann, and K. Reichmann, Electric field-induced changes of domain structure and properties in La-doped PZT. From ferroelectrics towards relaxors. *J Eur Ceram Soc*. **36**, 2495–2504 (2016).
- [8] G. H. Haertling, and C. E. Land, Hot-Pressed (Pb,La)(Zr,Ti) $\text{O}_3$  ferroelectric ceramics for electro-optic applications. *J Am Ceram Soc*. **54**, 1–11 (1971).
- [9] A. Sternberg, and A. Krumins, Transparent Ferroelectric Ceramics I. Composition, Structure and Requirements for Production. In: *Electro-Optic and Photorefractive Materials*, Springer-Verlag (Springer Proceedings in Physics). **18**, 50–60 (1987).
- [10] V. V. Shvartsman, A. L. Kholkin, A. Orlova, D. Kiselev, A. A. Bogomolov, and A. Sternberg, Polar nanodomains and local ferroelectric phenomena in relaxor lead lanthanum zirconate titanate ceramics. *Appl Phys Lett*. **86**, 202907 (2005).
- [11] D. A. Kiselev, I. K. Bdikin, E. K. Selezneva, K. Bormanis, A. Sternberg, and A. L. Kholkin, Grain size effect and local disorder in polycrystalline relaxors via scanning probe microscopy. *J Phys D*. **40**, 7109 (2007).
- [12] D. A. Kiselev, E. A. Neradovskaya, A. P. Turygin, V. V. Fedorovych, V. A. Shikhova, M. M. Neradovskiy, A. Sternberg, V. Ya. Shur, and A. L. Kholkin, Effect of surface disorder on the domain structure of PLZT ceramics. *Ferroelectrics*. **509**, 19–26 (2017).
- [13] V. Ya. Shur, E. L. Rumyantsev, G. G. Lomakin, O. V. Yakutova, D. V. Pelegov, A. Sternberg, and M. Kosec, AC switching of relaxor PLZT ceramics. *Ferroelectrics*. **314**, 245–253 (2005).
- [14] V. Ya. Shur, G. G. Lomakin, E. L. Rumyantsev, O. V. Yakutova, D. V. Pelegov, A. Sternberg, and M. Kosec, Polarization reversal in heterophase nanostructures: relaxor PLZT ceramics. *Phys Solid State*. **47**, 1340–1345 (2005).
- [15] V. Ya. Shur, G. G. Lomakin, V. P. Kuminov, D. V. Pelegov, S. S. Beloglazov, S. V. Slovikovskii, and I. L. Sorkin, Fractal-cluster kinetics in phase transformations in relaxor ceramic PLZT. *Phys Solid State*. **41**, 453–456 (1999).
- [16] J. F. Ihlefeld, J. R. Michael, B. B. McKenzie, D. A. Scrymgeour, J. P. Maria, A. P. Elizabeth, and A. R. Kitahara, Domain imaging in ferroelectric thin films via channeling-contrast backscattered electron microscopy. *J Mater Sci*. **52**, 1071–1081 (2017).
- [17] V. Ya. Shur, A. I. Lobov, A. G. Shur, S. Kurimura, Y. Nomura, K. Terabe, X. Liu, and K. Kitamura, Rearrangement of ferroelectric domain structure induced by chemical etching. *Appl Phys Lett*. **87**, 022905 (2005).
- [18] H. Kianirad, A. Zukauskas, C. Canalias, and F. Laurell, Domain dynamics in stoichiometric lithium tantalate revealed by wet etching and on-line second harmonic generation. *J Appl Phys*. **121**, 184103 (2017).
- [19] X. Yuhuan, *Ferroelectric Materials and Their Applications*, North-Holland, 1991.
- [20] T. Doi, E. Uhlmann, and I. Marinescu, *Handbook of Ceramics Grinding and Polishing*, Elsevier, 2015.
- [21] S. Mancha, Chemical etching of thin film PLZT. *Ferroelectrics* **135**, 131–137 (1992).

- [22] D. S. Chezganov, E. O. Vlasov, M. M. Neradovskiy, L. V. Gimadeeva, E. A. Neradovskaya, M. A. Chuvakova, H. Tronche, F. Doutre, P. Baldi, M. P. De Micheli, and V. Ya. Shur, Periodic domain patterning by electron beam of proton exchanged waveguides in lithium niobate. *Appl Phys Lett.* **108**, 192903 (2016).
- [23] D. K. Kuznetsov, D. S. Chezganov, E. A. Mingaliev, M. S. Kosobokov, and V. Ya. Shur, Visualization of nanodomain structures in lithium niobate and lithium tantalate crystals by scanning electron microscopy. *Ferroelectrics* **503**, 60–67 (2016).
- [24] J. Feder, *Fractals*, New York: Plenum Press, 1988.
- [25] V. V. Shvartsman, B. Dkhil, and A. L. Kholkin, Mesoscale domains and nature of the relaxor state by piezoresponse force microscopy. *Annu Rev Mater Res.* **43**, 423–449 (2013).
- [26] J. Cazaux, Charging in scanning electron microscopy «from inside and outside». *Scanning.* **26**, 181–203 (2004).
- [27] E. I. Rau, E. N. Evstaf'eva, and M. V. Andrianov, Mechanisms of charging of insulators under irradiation with medium-energy electron beams. *Phys Solid State* **50**, 621–630 (2008).